Design, Microfabrication, and Analysis of SAW RFID Tag

Henrique M. Vasconcelos, Member, IEEE, and Edval J. P. Santos, Senior Member, IEEE,
Laboratory for Devices and Nanostructures,
Centro de Tecnologia e Geociências - Escola de Engenharia de Pernambuco,
Universidade Federal de Pernambuco. Rua Acadêmico Hélio Ramos, s/n, Várzea,
50740-530, Recife, PE, Brasil. Email: edval@ee.ufpe.br

***Abstract*—Surface Acoustic Wave, SAW, Radio-Frequency Identification, RFID, tags have been fabricated on 128^o Y-cut lithium niobate wafers. The RFID system consists basically of a set of tags and one or more reader units. Each tag is responsible for carrying a unique identification code. As it uses radio waves, it is not required to have an unobstructed line-of-sight view between reader and tag, unlike the optical approach. Besides, RFID may not require a human operator. Other advantages of the SAW RFID tags include: truly passive operation, multiple tags can be read by a single interrogation pulse, and possible combination of identification and sensor capabilities. In this paper, the design and fabrication of SAW RFID tags are presented. The characterization was performed in frequency and time domain.**

***Keywords*—SAW, RFID, tag**

I. Introduction

The fundamental physical phenomenon lying behind surface acoustic wave, SAW, devices is piezoelectricity [1]. The interdigitated transducer, IDT, is used as the transducing element to excite acoustic waves and to collect the electrical signal. Basically, the SAW radio-frequency identification, RFID, tag works like a SAW delay line partially reflecting the interrogating pulse signal, as illustrated in Figure 1. The tag identity code returns as a pattern of echoes according to an encoding method based on the positions of the reflecting structures placed upon the piezoelectric substrate [2].

The antenna on the reader side radiates an RF interrogating pulse which is detected by the antenna attached to the tag. This electrical pulse is transformed into an acoustic pulse by the IDT. The generated acousto-electric pulse propagates along the substrate and interacts with the reflector array. Each reflector is precisely positioned to create an unique pattern of reflected signals back to the IDT. This train of reflected signals carries the tag identification code. The encoded reflected train of pulses is then converted back into the electrical form by the IDT, radiated by the antenna, and captured by the reading device. The received signal contains information about the amount and position of the reflectors in each tag [3].

Environmental variables, such as temperature and pressure, interact with the substrate, affecting its properties and changing the surface wave propagation characteristics. Thus, the SAW RFID tag can also be used as a sensor for remote measurement of physical and chemical quantities [4], [5]. A processor on the reader side should be able to measure the relative time delay between pulses and to associate any change to the specified physical or chemical quantity.

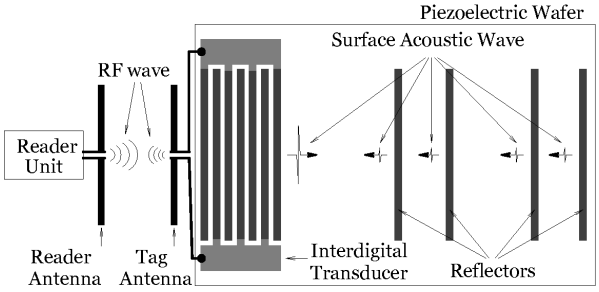

Figure 1. Principle of operation of the SAW RFID tag. Reading unit, antennas, IDT structure and reflector grating.

A unique identification code is associated with the positioning of the reflecting structures. As the train of echoes gets to the reading unit, the coded signal pattern corresponds to the position of each reflector. The code is based on the relative time delays between the reflected pulses, this method is called time position encoding. Another approaches are amplitude and phase of the reflected pulses [2]. The approach used can affect the interrogation range, the reader processing complexity and the realizable number of different id tags [3].

In time position encoded tags, the reflector grating is divided into groups with fixed time slots. The groups must have one reflecting structure which may occupy a single slot. The slot time is made equal to the interrogation pulse time width. The first time slot in each group must be left empty to avoid possible pulse overlap of reflected waves by adjacent reflectors. It is useful to place calibration reflectors to indicate the beginning and the end of the grating and a dead-time delay between the IDT and the first reflector is also necessary.

In the example shown in Figure 2, the reflecting grating was divided into three groups with five time slots. Only one reflecting structure should be inside each group respecting the forbidden slot condition. Thus, each reflector has four possible positions. In this scheme, the achievable number of different tag identities is 4^3.

In this method, all tags have the same number of reflecting structures regardless of the identity code they carry, which makes it easier to design them with uniform amplitudes of the response signal [3].

In this work, SAW RFID test structures have been designed and fabricated on 128° rotated Y-cut lithium niobate wafers. The paper is divided into four sections, this introduction is

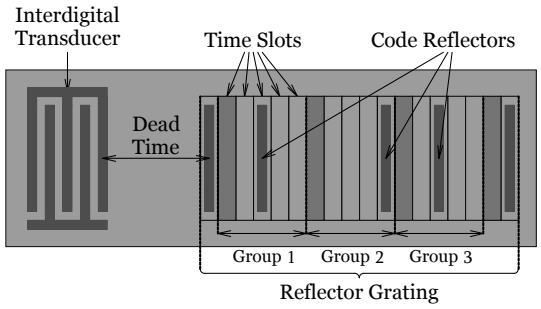

Figure 2. SAW RFID tag using time position encoding method.

the first. Next the methodology is presented. Thirdly, the discussion, and finally the conclusions.

II. Methodology

In this section, the design, fabrication and measurement of the RFID test structures are presented.

A. Design of Test Structures

To investigate the characteristics of the SAW RFID devices, test structures were designed as shown schematically in Figure 3. The devices are delay-line structures with varying parameters, such as number of finger pairs, N, and transducer separation distance, d. The aperture, L, is set to 5 mm. They were designed to allow for the measurement of transmission and reflection parameters in frequency domain and to perform delay-time measurement in the time domain.

The separation distance of an electrode pair is half the wavelength, $\lambda_0/2$, and the finger linewidth, $a = \lambda_0/4$. This wavelength determines the central operation frequency, $f_0 = v/\lambda_0$. The photolithographic process must be able to produce electrodes with such linewidth resolution. On the right side of Figure 3, two types of devices, designed for this work, are shown. The parameter values used are summarized in Table I. The expected sound speed for this wafer is 3970 m/s. This allows for the calculation of the expected center frequency.

Table I. Parameters for the test structures

Structure	λ_0	N	d	Reflectors
Delay line 1	40 μm	20	2 mm	none
Delay line 2	40 μm	40	2 mm	none
Delay line 3	40 μm	80	2 mm	none
Delay line 4	40 μm	20	3,6 mm	1
Delay line 5	40 μm	20	3,6 mm	3
Delay line 6	40 μm	20	3,6 mm	5
Delay line 7	40 μm	20	3,6 mm	7
Delay line 8	40 μm	20	3,6 mm	9

B. Device Microfabrication

The substrate material is a 3-inch diameter, 128° rotated, Y-cut lithium niobate wafer. After the wafer cleaning step, a thin 200-nm layer of aluminum was deposited by evaporation. The metalization step is performed before the photolithographic and etching steps. This is named *subtractive process*. The devices were fabricated using a one-step lithographic process as illustrated in Figure 4.

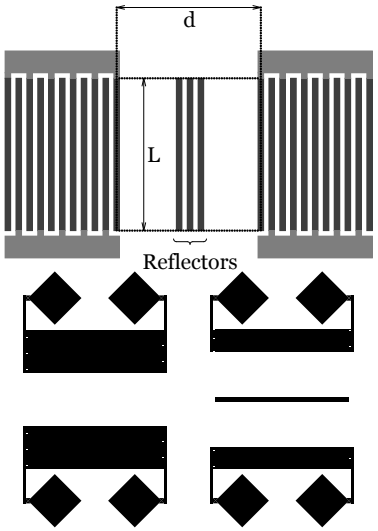

Figure 3. Geometry of the test structures, and two identical IDTs facing each other and separated by a distance, d. The IDT aperture, L, is 5 mm for all devices.

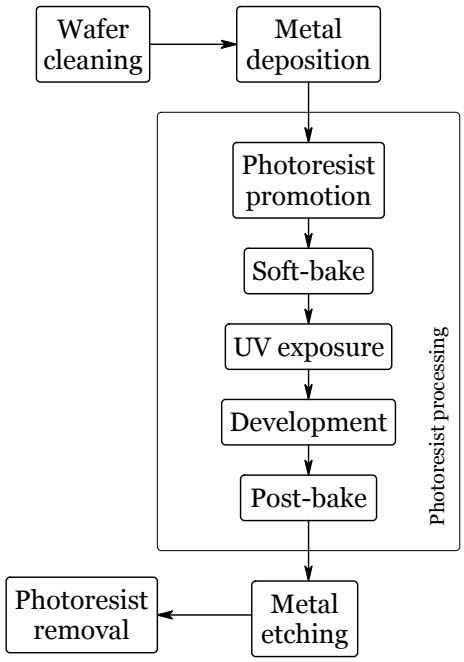

Figure 4. Microfabrication process flow.

The photoresist layer was applied by spin coating at 3000 rpm for one minute. After, the wafers are placed onto a hot plate for the soft-bake step at 90°C for one minute. The main purpose of this step is to evaporate residual solvent from the spun-on resist. Next, the UV exposure is performed, and the wafers are dipped into the developer, Shipley MF-319, for 30 s under agitation.

The last photoresist processing step is the post-bake process on the hot plate at 110°C for 1 minute. This step is required prior the etching process. The aluminium wet etching process was performed using a solution of equal parts of phosphoric acid, nitric acid and DI water. The solution temperature was

kept at 50°C. Finally, the wafer are rinsed in a DI water bath to stop the etching process, blown dry with nitrogen. The remaining photoresist on the wafer is removed with acetone. The fabricated devices are presented in Figure 5.

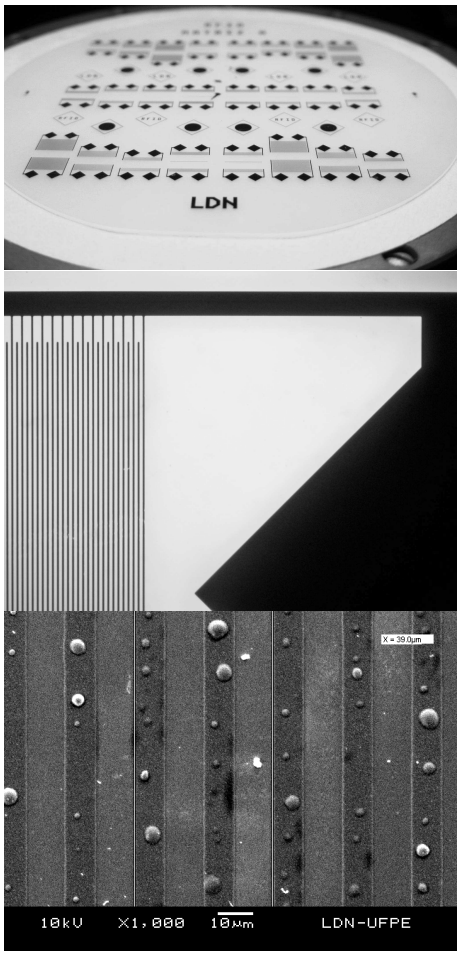

Figure 5. Top: LiNbO_3 wafer with fabricated IDT devices. Center: close-up view of one device, the linewidth achieved is 8 μm. Bottom: SEM image of fabricated device.

C. Measurement Results

To verify the operation of the SAW delay line, transmission and reflection parameters measurements were performed with a network analyzer, HP 8713T. An example of such measurement is presented in Figure 6. The central frequency is $f_0 = 91.2$ MHz.

The bandwidth of an interdigitated transducer is defined as the distance between the first two zeros around the central frequency of the the transfer function [6]. It can be estimated as $\Delta f = \frac{2f_0}{N}$.

As can be seen in Figure 7, increasing the number of pairs, N, reduces the device bandwidth, as expected. For all fabricated devices the center frequency is f_0 = 91.2 MHz. This yields a sound speed of 3557 m/s, for the direction the devices were fabricated. This result is below the expected speed.

To perform the time domain measurements, an RF-pulse was generated by mixing the RF signal with frequency f_0 with

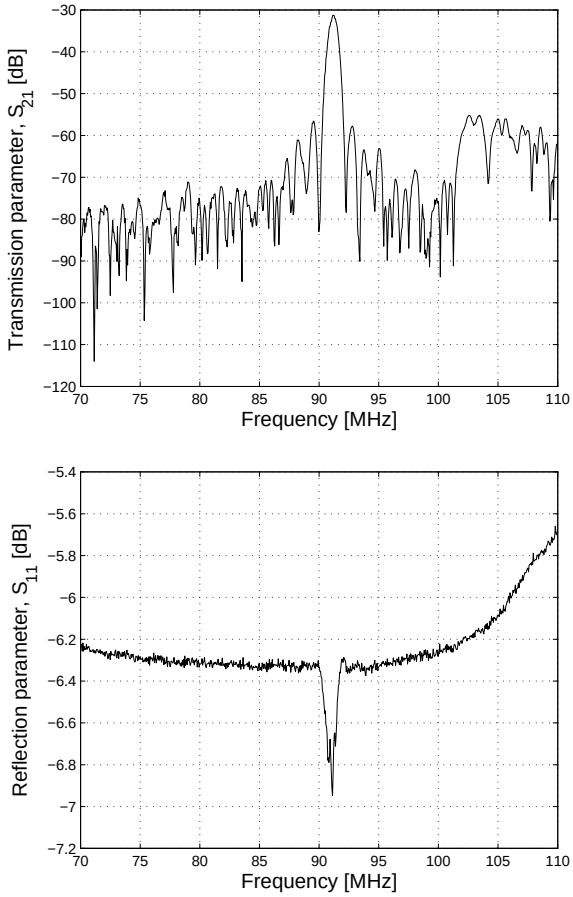

Figure 6. Transmission S_{21} and reflection S_{11} parameters extracted from a delay line with $N = 80$. The central frequency is $f_0 = 91.2$ MHz.

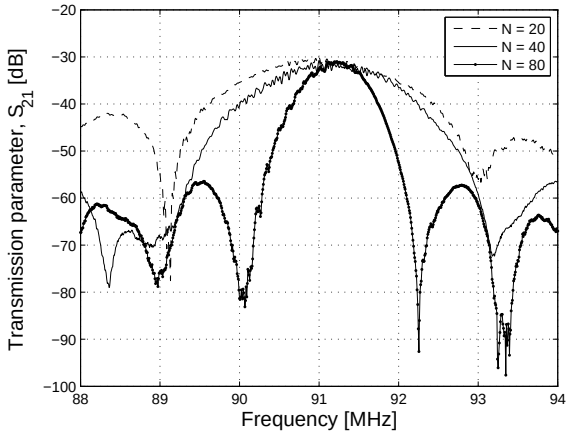

Figure 7. Delay line S_{21} transmission parameter as a function of the number of interdigitated pairs.

a pulse. This is a single port measurement. The generated pulse is injected in the same port used to capture the SAW echoes. The signals can be visualised with an oscilloscope.

The pulse was created with a function generator, starting with a 3-V, 125-kHz, square wave, and adjusting the duty cycle. The sinusoidal wave frequency was 91.2 MHz with an amplitude of 12 dBm.

For the Delay line structures without any electrodes in the path (DL 1, 2 and 3) a single echo due to the reflection of second IDT reflection is visualised. In Figure 8, the trace on top is the response of a delay line with 9 electrodes in the path between the two IDTs. The one in the bottom has no reflector between the two IDTs. Other echoes generated by multiple reflections may occur with smaller amplitude.

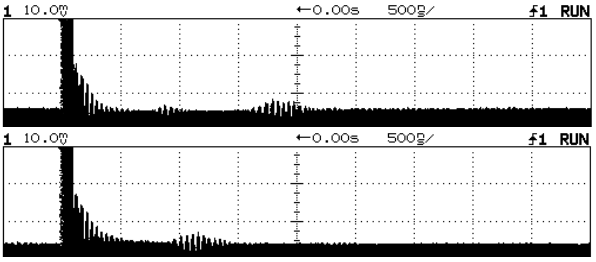

Figure 8. Different time responses for the two delay lines. On the top is the response of delay line with 9 electrodes in the middle of the two IDTs path. The one in the bottom has no reflector between the two IDTs with N =20.

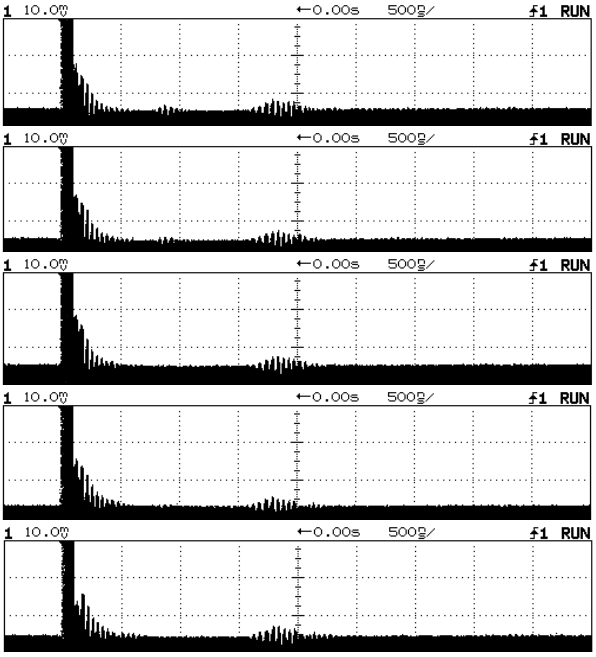

Figure 9. Time responses of the structures with 1, 3, 5, 7 and 9 electrodes in the middle of the path. On the top shows the response with 9 electrodes. Each electrode is a 10 μm aluminum strip.

III. Discussion

Considering the rightmost design in Figure 3, two echoes should be present, a strong one, which refers to the second IDT, and a weaker reflection in the middle which refers to the position of the reflector. Each time delay response can be calculated as shown in Equation 1.

$$\Delta t_i = \frac{2 \times d_i}{v_{saw}} \tag{1}$$

The time delays for the two structure types are summarized in Table II, using the extracted speed, $v_{saw} = 3557$ m/s.

Table II. Expected response time delays

Structure	d_i	Δt_i
DL 1,2,3	$d_1 = 1.95$ mm	$\Delta t_1 = 1096.2$ ns
DL 4,5,6, 7 and 8	$d_1 = 1.755$ mm $d_2 = 3.51$ mm	$\Delta t_1 = 986.6$ ns $\Delta t_2 = 1973.2$ ns

As expected, increasing the number of electrodes in the reflector, one gets more reflected power. This is observed on the right side of Figure 8. Different number of electrodes (4, 5, 6, 7 and 8) are placed in the middle.

IV. Conclusion

SAW RFID tags have been successfully fabricated by applying a subtractive process. The devices were characterized in both frequency and time domain. The calculated acoustic speed was not as expected and a new wafer is being prepared to confirm this result. Further improvements in the time-domain setup is required to get higher time resolution, necessary to capture the encoded pattern. Further developments in design and fabrication may reduce resistive losses, and diffraction effects. Encoding strategies may also improve device performance.

Acknowledgment

The authors are thankful to FINEP, PETROBRAS, and CNPq.

References

[1] David P. Morgan, *History of SAW devices*, IEEE International Frequency Control Symposium, 1998.

[2] V. P. Plessky, *Review on SAW RFID tags*, IEEE Transactions on Ultrasonics, Ferroelectrics, and Frequency Control, Vol. 57, No. 3, March 2010, pp. 654-668.

[3] S. Hrm, W. G. Arthur, C. S. Hartmann, R. G. Maev, V. P. Plessky, *Inline SAW RFID tag using time position and phase encoding*, IEEE Transactions on Ultrasonics, Ferroelectrics, and Frequency Control, Vol. 55, No. 8, August 2008, pp. 1840-1846.

[4] G. Bruckner, R. Hauser, L. Maurer, L. Reindl, R. Teichmann, J. Biniasch, *High temperature stable SAW based tagging system for identifying a pressure sensor*, IEEE Proc. of the 2003 IEEE International Frequency Control Symposium and PDA Exhibition, May 2003, pp. 943-947.

[5] F. Schmidt, O. Sczesny, L. Reindl, V. Mgori, *Remote sensing of physical parameters by means of passive surface acoustic wave devices (ID-tag)*, Proc. IEEE Ultrasonics Symposium, pp. 589-592, Cannes, France, November 1994.

[6] W. R. Smith, H. M. Gerard, J. R. Collins, T. M. Reeder, H. J. Shaw, *Analysis of interdigital surface wave transducers by use of an equivalent circuit model*, IEEE Transactions on Microwave Theory and Techniques, vol. MTT-17, pp. 856-864, November 1969.